



HAL
open science

Correlative imaging of single carbon nanotubes and fluorescently labelled neuronal structures in the extracellular space of live brains

Chiara Paviolo, Joana S Ferreira, Antony Lee, Laurent Groc, Laurent Cognet

► **To cite this version:**

Chiara Paviolo, Joana S Ferreira, Antony Lee, Laurent Groc, Laurent Cognet. Correlative imaging of single carbon nanotubes and fluorescently labelled neuronal structures in the extracellular space of live brains. SPIE Photonics Europe - Neurophotonics, Apr 2020, Strasbourg, France. hal-03297940

HAL Id: hal-03297940

<https://hal.science/hal-03297940v1>

Submitted on 23 Jul 2021

HAL is a multi-disciplinary open access archive for the deposit and dissemination of scientific research documents, whether they are published or not. The documents may come from teaching and research institutions in France or abroad, or from public or private research centers.

L'archive ouverte pluridisciplinaire **HAL**, est destinée au dépôt et à la diffusion de documents scientifiques de niveau recherche, publiés ou non, émanant des établissements d'enseignement et de recherche français ou étrangers, des laboratoires publics ou privés.

Correlative imaging of single carbon nanotubes and fluorescently labelled neuronal structures in the extracellular space of live brains

Chiara Paviolo^a, Joana S. Ferreira^b, Antony Lee^a, Laurent Groc^b, Laurent Cagnet^a

^aUniversité de Bordeaux, Institut d'Optique & Centre National de la Recherche Scientifique, UMR 5298, 33400 Talence, France; ^bUniversité de Bordeaux, Interdisciplinary Institute for Neuroscience, UMR 5297, 33076 Bordeaux

ABSTRACT

The brain extracellular space (ECS) is a complex network that constitutes a key microenvironment for cellular communication, homeostasis, and clearance of toxic metabolites¹. Signaling molecules, neuromodulators, and nutrients transit via the ECS, therefore mediating the communication between cells. Despite the relevance of this important part of the brain, its dynamics and structural organization at the nanoscale is still mostly unknown². We have recently demonstrated that single-walled carbon nanotubes (SWCNTs) can be used to image and probe live brain tissue, providing super-resolved maps of the brain ECS and quantitative information on the local diffusion environment^{3,4}. Here, we propose an important refinement of this approach by implementing a structured illumination technique (named HiLo microscopy⁵) to image fluorescently labelled neuronal structures in parallel to SWCNT NIR imaging. This technique is based on speckle illumination and relies on the acquisition of one structured and one uniform illumination image to obtain images deep into tissues with good optical sectioning. Having access to spatially resolved SWCNT diffusivity around specific neuronal structures will provide more precise insights about the heterogeneity of the brain environment.

Keywords: Single-walled carbon nanotubes, super-resolution microscopy, brain extracellular space, live brain imaging, neuronal structures, HiLo microscopy

1. INTRODUCTION

The extracellular space (ECS) is a complex network of biomolecules that constitutes a key microenvironment for cellular communication, homeostasis, and clearance of toxic metabolites¹. In the brain, its spatial organization varies during sleep⁶, development⁷, and aging⁸, and it is probably altered in neuropsychiatric and degenerative diseases⁹. Signaling molecules, neuromodulators, and nutrients transit via the ECS, therefore mediating the communication between cells¹. Molecules present in the ECS also regulate various aspects of synaptic plasticity, such as scaling of synaptic responses, metaplasticity and stabilization of synaptic connectivity¹⁰. Despite the relevance of this important part of the brain, its dynamics and structural organization at nanoscale temporal and spatial resolution still represent a knowledge frontier in brain research².

To date, the main methodologies to study the ECS are electron microscopy¹¹ and macroscopic biophysical investigations, such as radiotracer measurements, real-time iontophoresis and integrative optical imaging². Both techniques present several drawbacks, due to the intrinsic difficulties for simultaneously studying the ECS local topology and dynamics at the nanoscale. These include: *i*) the poor preservation of the fine structures of the extracellular space and matrix due to the chemical fixative method¹¹ or the invasiveness of the measurement technique², *ii*) the loss of the probe during the quantification of the ECS rheological properties because of the blood-brain barrier or cellular uptake and binding, and, importantly, *iii*) an often inadequate spatial resolution which is not suitable to correctly represent the ECS nanoscale network. Recently, a super-resolution shadow imaging based on 3D-STED microscopy (SUSHI) was developed to visualize the structure and dynamics of the ECS in response to different physiological stimuli¹². Although this technique gave unprecedented information on the micro-anatomical organization of live brain structures, the methodology is limited in penetration depth in biological tissues and does not provide information about ECS molecular diffusion.

*laurent.cagnet@u-bordeaux.fr;

To access deeper intact brain tissue and measure diffusion processes in the ECS, we have recently demonstrated that single-walled carbon nanotubes (SWCNTs) can be used to image and probe live brain tissues, providing super-resolved maps of the brain ECS and quantitative information on the local diffusion environment^{3,4}. SWCNTs are stiff quasi-one-dimensional tubular all-carbon nanostructures, with diameters of ~1 nm and variable lengths (from hundreds of nm to several μm). This unusual length-to-diameter aspect ratio enhances their penetration in complex environment, while the combination of their length and rigidity can moderate their diffusion rates to be compatible with video-rate for single-molecule imaging¹³. Individual semiconducting SWCNTs exhibit luminescence with large Stokes shifts in the near-infrared (NIR) window (typically ca. 900 to 1400 nm). This range not only falls in the therapeutic window of biological tissues (typically ca. 650 to 1400 nm), but it is also potentially free of autofluorescence coming from biological structures¹⁴. The fluorescence emission of SWCNTs is highly stable and displays no blinking and negligible photobleaching, allowing long-term tracking in biological tissues (tens of minutes). In our previous work, SWCNTs were imaged in live brain slices of both young and adult rodent brain⁴. Tracking of SWCNTs provided unique simultaneous information on local nanoscale ECS dimensions and diffusion environments, revealing a maze of polymorphic compartments bearing specific rheological properties. It is now key to correlate the localization of SWCNTs with morphological information of the brain tissue. Many cellular structures can be labelled using fluorescent markers, however a specialized imaging technique needs to be built up as a standard widefield microscope does not provide enough resolution to reveal structures deep into a biological tissue.

Here, we implement a previously designed structured illumination technique (named HiLo microscopy⁵) in parallel to SWCNT NIR imaging to study morphological and diffusion properties of the brain ECS around fluorescently labeled presynaptic regions. HiLo implies the acquisition of one structured and one uniform illumination image to obtain by post-acquisition analysis images with good optical sectioning. In our work, the structured illumination is based on speckle illumination. With our multimodal acquisition system we managed to merge on the same setup single molecule tracking and optically sectioned imaging in live biological samples.

2. MATERIALS AND METHODS

2.1 HiLo setup

The HiLo microscope was implemented on a standard upright microscope (Nikon) used to image SWCNT diffusion. For HiLo, a 568 nm laser source is used to excite the fluorescence of neuronal structures. The laser speckles for structured illumination were obtained with a static optical diffuser (Thorlabs). The beam was initially expanded with lenses L1 and L2 before illuminating the diffuser (Figure 1A). Images were acquired alternating uniform (I_u) and speckle (I_s) illuminations. HiLo images were calculated thereafter using a program developed in-house using MATLAB and following the procedure of Lim *et al*⁵. Briefly, the local contrast (C_z) was directly estimated in the difference between the speckle and uniform image ($I_s - I_u$). This parameter acts as a weighting function that is peaked when the object is in-focus and decays to zero as the object goes out-of-focus. A low-resolution estimate of the in-focus image (I_{LP}) is then constructed by applying a lowpass filter (LP) to the weighted uniform illumination image, obtaining:

$$I_{LP} = LP [C_z I_u] \quad (1)$$

The complementary high-resolution information (I_{HP}) is obtained by applying a high-pass filter directly to the uniform illumination image. The final HiLo image is constructed from the fusion of the above two images, resulting in:

$$I_{HiLo} = \eta I_{LP} + I_{HP} \quad (1)$$

where η is a scaling function that ensures a smooth transition between low to high spatial frequencies.

2.2 Rat organotypic slices

Organotypic slice cultures were prepared as previously described⁴. Hippocampal slices (350 μm) were obtained from postnatal day 5 to postnatal day 7 Sprague-Dawley rats using a McIlwain tissue chopper and then placed in warm dissection medium containing (in mM): 175 sucrose, 25 D-glucose, 50 NaCl, 0.5 CaCl₂, 2.5 KCl, 0.66 KH₂PO₄, 2 MgCl₂, 0.28 MgSO₄-7H₂O, 0.85 Na₂HPO₄-12H₂O, 2.7 NaHCO₃, 0.4 HEPES, 2 \times 10⁻⁵% phenol red, pH 7.3. After 25 min of incubation, slices were transferred to hydrophilic polytetrafluoroethylene (FHLC) membranes (Millipore) set on Millicell Cell Culture Inserts (Millipore) and cultured for up to 14 days at 35°C / 5% CO₂ in a culture medium composed of 50% Basal Medium Eagle, 25% Hank's balanced salt solution, 25% horse serum, 0.45% D-glucose, and 1mM L-glutamine.

2.3 HiLo characterization

To validate the optical sectioning of the HiLo microscope, a fluorescent layer of Alexa 647 (Thermo Fisher) in polyvinylpyrrolidone (3% PVP, 1:1 ratio) was spin coated onto glass coverslips (# 1.5, Menzel-Gläser GmbH) at 920 rpm. Two different coverslips were then separated using a mechanical spacer, with the fluorescent layers facing each other (inset in Figure 1B). The space between the coverslips was filled with water. Images were taken using a long working distance water immersion 60× objective (NA 1.0, Nikon) and 200 ms exposure time. The resolution of the optical sectioning was calculated on four independent measurements. Data are presented as mean and standard deviation of the mean.

For validation of the technique with thick biological samples, brain slices were initially fixed for 2 hours in paraformaldehyde. A standard protocol for immunostaining was followed thereafter. Briefly, slices were incubated in 1% PBS-Triton-X100 and 4% BSA before antibody incubation. Tissues were then incubated overnight at 4 °C with allograft inflammatory factor 1 antibody (Iba1, Abcam) in 2% BSA PBS solution (1:200 dilution). The secondary antibody anti-Iba1 (goat anti-rabbit Alexa568, Wako Pure Chemical Industries) at 1:1000 dilution in PBS was then applied for 2 h at room temperature under agitation. Each step of the immunostaining was followed with three cycles of washing in PBS (5 min each wash). Images were taken using a long working distance objective (60×, NA 1.0, Nikon) with a 20 mW laser power and 200 ms exposure time.

HiLo was additionally validated in rat organotypic slices labelled for activated presynaptic terminals. Slices were transferred in HEPES-based artificial cerebrospinal fluid (aCSF) containing (in mM): 130 NaCl, 2.5 KCl, 2.2 CaCl₂, 1.5 MgCl₂, 10 HEPES, and 10 D-glucose, and incubated for 5 min with 20 μM of FM 4-64 lipophilic Styryl dye at 35 °C / 5% CO₂. Tissues were then stimulated for 5 min with 50 mM KCL, for the synaptic uptake of the dye. For excessive labeling removal, slices were successively washed in aCSF twice for 10 to 15 min. Tissues were returned to original dishes until imaging.

2.4 SWCNT preparation and incubation

SWCNTs were prepared as previously published with minor modifications⁴. Briefly, 1 mg of HiPco synthesized carbon nanotubes (from Rice University) was suspended with 50 mg of monofunctional phospholipid-polyethylene glycol (PL-PEG) molecules (#mPEG-DSPE-5000, Laysan Bio) in 10 ml of deuterium oxide (Sigma Aldrich). To individually disperse the nanotubes, a 15 min homogenization at 19,000 rpm followed by an 8 min tip sonication at 20W were applied to the solution. SWCNT bundles and impurities were further precipitated by centrifugation at 3,000 rpm for 60 min. 70–80% of the supernatant was then collected and stored at 4 °C.

SWCNTs were incubated in the slices 2 hours prior imaging. 3 μl of SWCNT solution was mixed with 100 μl of culture medium and incubated with the slices at 35 °C / 5% CO₂. Slices were imaged for up to 1 h in aCSF before being discarded.

2.5 SWCNT and synapse imaging

Imaging of diffusing SWCNTs in the ECS of rat organotypic cultures was performed on a customized epifluorescent microscope (Nikon) equipped with an EMCCD camera (ProEM-HS, Princeton Instrument). A 845 nm laser was used to excite the (6,5) SWCNTs at a phonon sideband ($\lambda_{\text{exc}} = 845 \text{ nm} / \lambda_{\text{em}} = 986 \text{ nm}$) with a circular polarized excitation. A standard 4× objective (NA 0.1, Nikon) was initially used to check the CA1 position in the hippocampal slice. Images were collected using a water immersion 60× objective (NA 1.0, Nikon) using an exposure time of 30 ms. HiLo microscopy for synapse visualization was performed at the end of each SWCNT recording.

2.6 Image analysis

Analysis of individual diffusing SWCNTs in the ECS of live tissues was performed as previously described with some modifications⁴. Briefly, the super-localization of the SWCNT centroids was obtained by fitting the images with two-dimensional asymmetric Gaussian functions having arbitrary orientations. Three consecutive images were averaged for each fit to improve the localization precision (~50 nm in water). SWCNT coordinates were then interconnected to reconstruct nanotube trajectories. Drift was removed using an immobile SWCNT in the field of view. For each trajectory, the SWCNT length was estimated using the distribution of the longest axis of the 2D asymmetric Gaussian fits for negligible SWCNT movements (displacements between consecutive images < 40 nm) corrected by the point-spread function of the microscope and the exciton diffusion length¹⁵.

The instantaneous mean square displacement (*MSD*) was also calculated for each trajectory as a function of time intervals Δt . For short time delays (90 ms), the two-dimensional *MSD* can be approximated by a linear slope,

$$MSD(t) = 4D_{inst}\Delta t \quad (3)$$

therefore allowing the definition of D_{inst} , the instantaneous diffusion coefficient. The local relative diffusivity was defined as the ratio between D_{inst} and the value of free diffusion (D_{ref}) that the considered SWCNT would have in a fluid bearing the viscosity of the cerebrospinal fluid (η_{ref}):

$$D_{ref} = \frac{3k_B T \ln(2\varphi)}{8\pi\eta_{ref}L} \quad (4)$$

where k_B is the Boltzmann constant., T is the temperature, φ is the SWCNT aspect ratio and L is the nanotube length. For visualization purposes, the spatial diffusivity maps were convoluted with a 2D Gaussian of 50 nm full width at half maxima.

3. RESULTS

The optical setup for HiLo microscopy has been built up around a standard upright microscope also used for SWCNT imaging (Figure 1A). To achieve optical sectioning, a uniform widefield illumination (UWI) and a speckle illumination (SI) images were alternatingly acquired for each field of view (insets in Figure 1A). The SI was obtained when a diffuser was positioned on the laser path. To quantify the optical sectioning of the HiLo setup, z -stacks of two fluorescent layers of Alexa 647 spaced of $\sim 250 \mu\text{m}$ were recorded in both conditions (Figure 1B). UWI only detected broad fluorescent axial distributions, which did not allow to recover the position of the fluorescent layers. On the other side, HiLo microscopy clearly distinguished the two separate coatings, showing sharp peaks of fluorescence at 35 and 280 μm axial positions. The full width at half maximum of the peaks proved to be $9.5 \pm 2.4 \mu\text{m}$. Fixed brain slices stained for Iba1 were then used to demonstrate the capability of the microscope for optical sectioning in high-scattering biological samples (Figure 1C). The HiLo microscope revealed the expression of the proteins on individual cells, not distinguishable in UWI. The optical sectioning of the technique was further demonstrated by the 3D reconstruction of a z -stack, which confirmed the localization of the staining in different cell compartments. HiLo microscopy also proved the removal of the background fluorescence coming from out-of-focus optical layers. The capability of the technique was finally tested on its ability to image active presynaptic terminals of rat organotypic slices labelled with FM 4-64 dyes (Figure 1D). The in-built HiLo microscope allowed to distinguish and localize individual synapses at different depths in the tissue, which standard widefield imaging could not reveal. This confirmed the removal of the background fluorescence for live high-scattering biological samples.

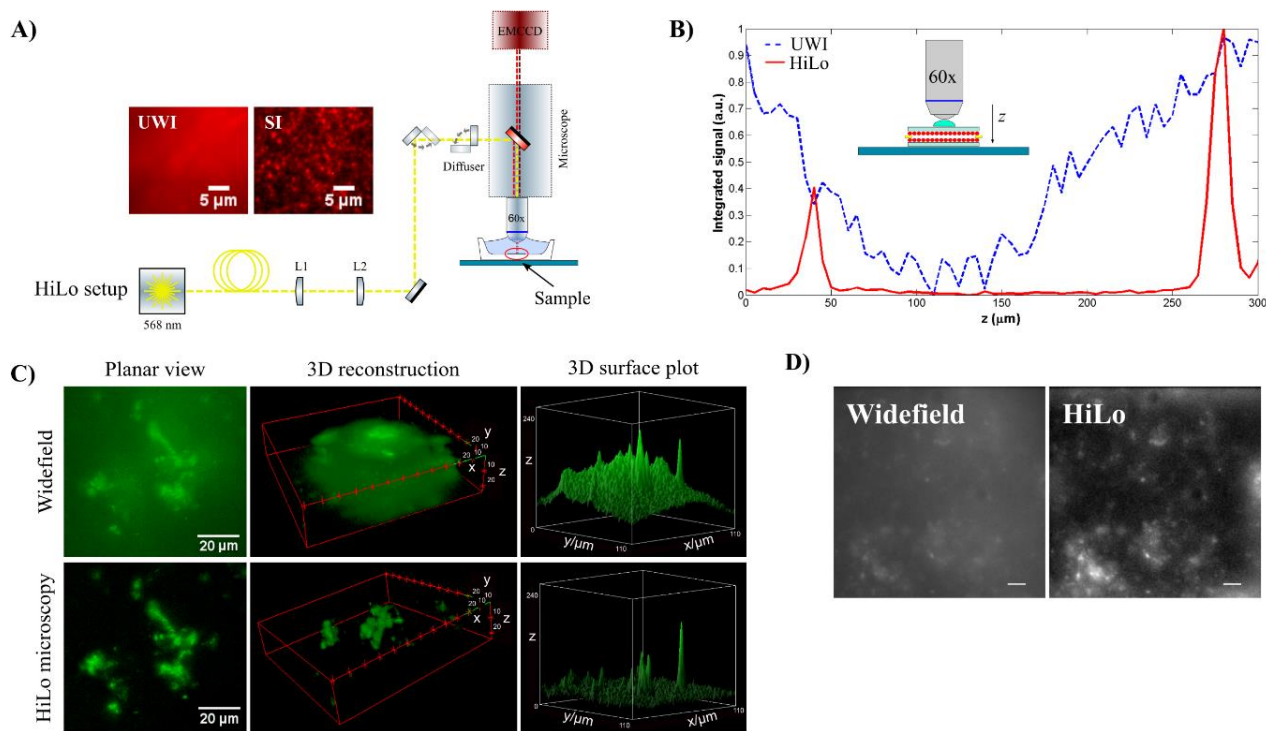


Figure 1. Schematic and characterization of the HiLo setup. A) A 568 nm laser was expanded with lenses L1 and L2 before reaching a static diffuser. Fluorescent images were acquired with an EM-CCD camera. Insets are fluorescent Alexa 647 layers imaged with uniform widefield (UWI) and speckle illumination (SI). B) Two Alexa 647 layers can be distinguished in HiLo microscopy (solid red line), while they appeared as broad peaks in UWI (dotted blue). C) Comparison of standard widefield and HiLo microscopy (planar view, 3D reconstruction and surface plot) in a brain slice stained for Iba1. The HiLo microscope revealed the expression of the proteins on individual cells and confirmed the removal of the out-of-focus background fluorescence. Scale bars are 20 μm . D) Comparison of standard widefield and HiLo microscopy on a rat organotypic slice stained for active presynaptic terminals. Scale bars are 5 μm .

HiLo microscopy was then applied in parallel to SWCNT imaging to correlate the localizations of the NTs with morphological information of the brain tissue (Figure 2A). SWCNTs were initially functionalized with PL-PEG molecules, to prevent non-specific biomolecule adsorption and minimize their sticking onto biologicals structures. The first 10 μm of tissue were discarded to exclude the first cell layers potentially damaged by the preparation. SWCNTs showed high photoluminescence stability (Video 1). The continuous NIR excitation did not evidence photobleaching of the nanoprobe. The correlation of the visible (i.e. synapses) and the NIR (i.e. SWCNTs) images gave indication of SWCNT presence in the proximity of these key neuronal structures (insets in Figure 2A).

Freely moving SWCNTs in the brain ECS were detected for several minutes at different depths in the tissue and up to 70 μm (Figure 2B). For each recorded frame, the 2D Gaussian fitting analysis allowed the extraction of the nanotube centroids with subwavelength precision (~ 50 nm). Moreover, the asymmetric Gaussian fits gave information on the distribution of the SWCNT length (Figure 2B). The length distribution was centered on 500 nm with very few outliers, confirming the consistency and reproducibility of the nanotube preparation. Reconstructed trajectories (example in Figure 2C) gave an indication of the total area of SWCNT activity. On a total of 20 SWCNTs and with an average recording time of 2.5 minutes, nanotubes explored on average $\sim 17 \mu\text{m}^2$ with a peak of $\sim 50 \mu\text{m}^2$ (Figure 2C). Maps on local diffusivities ($D_{\text{ins}}/D_{\text{ref}}$, Figure 2D) were calculated using a 390 ms sliding window along the global MSDs, revealing spatially heterogeneous diffusion patterns depending on the rheological properties of the brain ECS.

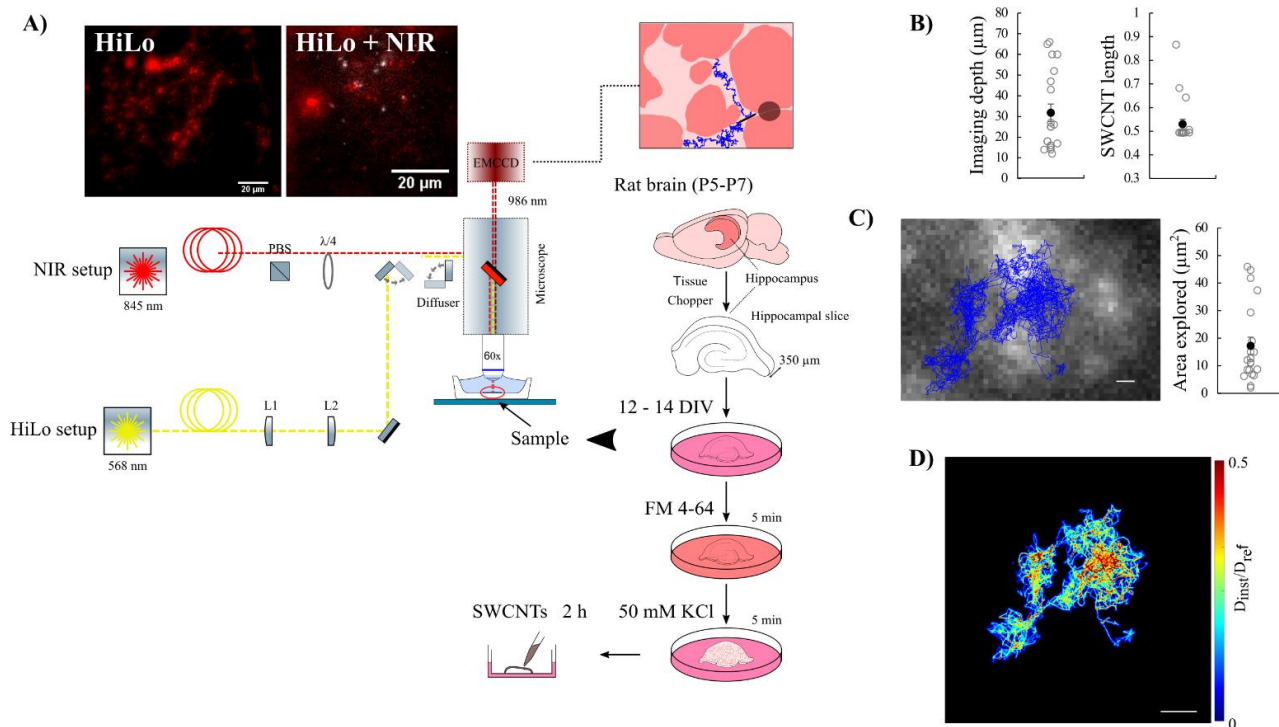


Figure 2. HiLo microscopy in parallel to NIR imaging. A) Schematic of the experimental setup. A NIR laser line with controlled circular polarization (PBS, polarization beam splitter) was added to the HiLo visible imaging. Rat organotypic slices were cultured for up to 14 days before being imaged. SWCNTs were incubated for 2 h at 35°C / 5% CO₂ before each experiments. Insets are an example of active presynaptic terminals imaged with HiLo microscopy (red) and in combination with SWCNT NIR imaging (white). B) Graph of imaging depth and SWCNT length for 20 independent experiments. Data are expressed as mean \pm standard error of the mean. C) Example of a trajectory retrieved after the 2D Gaussian fitting of the SWCNT localizations (~ 5000 points). Scale bar is 1 μm . Graph represents the area explored by tracked SWCNTs during 20 independent recordings. Data are expressed as mean \pm standard error of the mean. D) Example of the instantaneous diffusivity map from the trajectory presented in (C). Scale bar is 2 μm .



Video 1. Example of SWCNTs in rat organotypic slices. Scale bar is 5 μm . <http://dx.doi.org/doi.number.goes.here>

4. DISCUSSION

This study presents the implementation of a HiLo microscope in parallel to NIR imaging to correlate the localizations of freely moving SWCNTs with morphological information of the brain tissue. HiLo microscopy is indeed a powerful technique, and has already been applied to image different biological samples⁵ and for functional imaging of calcium

dynamics¹⁶. Here, HiLo microscopy allows the correlation of the synaptic positions with areas of SWCNT activity in the ECS of live brain tissues.

HiLo was implemented on a standard widefield microscope and was validated on different biological specimens/molecular probes. The technique presented a high versatility and reproducibility, and can be easily extended to target different morphological features of the biological tissues (e.g. by labelling the components of the extracellular matrix). The in-built setup achieved optical sectioning both in fixed and live brain tissues. When combined with single particle tracking of SWCNTs, HiLo allowed the visualization of active presynaptic regions in live tissue, which standard widefield illumination could not reveal. Moreover, SWCNTs were used to explore the live brain ECS, giving information on the diffusivity environment at the nanoscale level. Importantly, SWCNTs can be tracked in live brain tissues for several minutes, showing negligible photobleaching and/or tissue damage, providing the opportunity to image specific events when the nanotubes approach the fluorescently labeled structures identified by HiLo. Having access to spatially resolved SWCNT diffusivity around specific neuronal structures will provide novel insights about the heterogeneity of the environment, which macroscopic methods cannot reveal. This work opens up novel opportunities to unveil the fundamental characteristics of the brain ECS.

5. CONCLUSIONS

This study presents a simple, easy-to-implement and cost-efficient method to achieve optical sectioning in thick high-scattering samples. HiLo microscopy in combination with deep-tissue super-localization microscopy represent a unique approach in neuroscience, paving the way to probe adult brain tissues in aging and neurological disorders. Moreover, single-nanotube tracking together with other labelling strategies will enable targeting specific unexplored compartments, such as the synaptic cleft or the perineuronal milieu.

6. ACKNOWLEDGEMENTS

C.P. acknowledges funding from the European Union's Horizon 2020 research and innovation program under the Marie Skłodowska-Curie grant agreement No 793296. This work was specifically supported by grants from the Agence Nationale de la Recherche (ANR-14-OHRI-0001-01, ANR-15-CE16-0004-03), IdEx Bordeaux (ANR-10-IDEX-03-02), the France-BioImaging national infrastructure (ANR-10-INBS-04-01), and the Labex Brain Program (ANR-10-LABX-43). Animal experiments were performed at the Animal Facilities of the University of Bordeaux, supported by the Région Nouvelle-Aquitaine.

REFERENCES

- [1] Syková, E. and Nicholson, C., “Diffusion in brain extracellular space,” *Physiol. Rev.* **88**(4), 1277–1340 (2008).
- [2] Nicholson, C. and Hrabětová, S., “Brain extracellular space: the final frontier of neuroscience,” *Biophys. J.* **113**(10), 2133–2142 (2017).
- [3] Godin, A. G., Varela, J. A., Gao, Z., Danné, N., Dupuis, J. P., Lounis, B., Groc, L. and Cognet, L., “Single-nanotube tracking reveals the nanoscale organization of the extracellular space in the live brain,” *Nat. Nanotechnol.* **12**(3), 238–243 (2017).
- [4] Paviolo, C., Soria, F. N., Ferreira, J. S., Lee, A., Groc, L., Bezard, E. and Cognet, L., “Nanoscale exploration of the extracellular space in the live brain by combining single carbon nanotube tracking and super-resolution imaging analysis,” *Methods* (2019).
- [5] Lim, D., Ford, T. N., Chu, K. K. and Mertz, J., “Optically sectioned in vivo imaging with speckle illumination HiLo microscopy,” *J. Biomed. Opt.* **16**(1), 016014-016014–016018 (2011).
- [6] Xie, L., Kang, H., Xu, Q., Chen, M. J., Liao, Y., Thiyagarajan, M., O’Donnell, J., Christensen, D. J., Nicholson, C., Iliff, J. J., Takano, T., Deane, R. and Nedergaard, M., “Sleep drives metabolite clearance from the adult brain,” *Science* **342**(6156), 373–377 (2013).
- [7] Lehmenkühler, A., Syková, E., Svoboda, J., Zilles, K. and Nicholson, C., “Extracellular space parameters in the rat neocortex and subcortical white matter during postnatal development determined by diffusion analysis,” *Neuroscience* **55**(2), 339–351 (1993).
- [8] Metzler-Baddeley, C., Jones, D. K., Belaroussi, B., Aggleton, J. P. and O’Sullivan, M. J., “Frontotemporal connections in episodic memory and aging: a diffusion MRI tractography study,” *J. Neurosci.* **31**(37), 13236–13245 (2011).
- [9] Berezin, V., Walmod, P. S., Filippov, M. and Dityatev, A., “Targeting of ECM molecules and their metabolizing enzymes and receptors for the treatment of CNS diseases,” *Prog. Brain Res.* **214**, 353–388 (2014).
- [10] Dityatev, A., Schachner, M. and Sonderegger, P., “The dual role of the extracellular matrix in synaptic plasticity and homeostasis,” *Nat. Rev. Neurosci.* **11**(11), 735–746 (2010).
- [11] Korogod, N., Petersen, C. C. H. and Knott, G. W., “Ultrastructural analysis of adult mouse neocortex comparing aldehyde perfusion with cryo fixation,” *Elife* **4** (2015).
- [12] Tønnesen, J., Inavalli, V. V. G. K. and Nägerl, U. V., “Super-resolution imaging of the extracellular space in living brain tissue,” *Cell* **172**(5), 1108-1121.e15 (2018).
- [13] Fakhri, N., MacKintosh, F. C., Lounis, B., Cognet, L. and Pasquali, M., “Brownian motion of stiff filaments in a crowded environment,” *Science* **330**(6012), 1804–1807 (2010).
- [14] Fakhri, N., Wessel, A. D., Willms, C., Pasquali, M., Klopfenstein, D. R., MacKintosh, F. C. and Schmidt, C. F., “High-resolution mapping of intracellular fluctuations using carbon nanotubes,” *Science* **344**(6187), 1031–1035 (2014).
- [15] Oudjedi, L., Parra-Vasquez, A. N. G., Godin, A. G., Cognet, L. and Lounis, B., “Metrological investigation of the (6,5) carbon nanotube absorption cross section,” *J. Phys. Chem. Lett.* **4**(9), 1460–1464 (2013).
- [16] Lauterbach, M. A., Ronzitti, E., Sternberg, J. R., Wyart, C. and Emiliani, V., “Fast calcium imaging with optical sectioning via HiLo microscopy,” *PLOS ONE* **10**(12), e0143681 (2015).